Theoretical and Experimental Motion Analysis of Self-Compensating Dynamic Balancer

Jongkil Lee*

(Received June 30, 1994)

A theoretical and experimental approach was used to investigate the motion and effectiveness of a Self-Compensating Dynamic Balancer (SCDB). This is a device intended to minimize the effects of rotor imbalance and vibratory forces on a rotating system during normal operation. The basic concept of an automatic dynamic balancer has been described in many U.S. patents. The SCDB is composed of a circular disk with a groove containing massive balls and low viscosity damping fluid. The objective of this research is to determine the motion of the balls and how this ball motion is related to the vibration of the rotating system using both theoretical and experimental methods. The equations of motion of the balls were derived by the Lagrangian method. Static and dynamic solutions were derived from the analytic model. To consider the dynamic stability of the motion, perturbation equations were investigated by two different methods : Floquet theory and direct computer simulation. On the basis of the results of the stability investigation, ball positions which result in a balance system are stable above the critical speed and unstable at critical speed and below critical speed. To determine the actual critical speed of the rotating system used in the experimental work, a modal analysis was conducted. Experimental results confirm the predicted ball positions. Based on the theoretical and experimental results, when the system operates below and near the first critical speed, the balls do not balance the system. However, when the system operates above the first critical speed the balls can balance the system.

Key Words : Self-Compensating Dynamic Balancer, Rotating Machinery, Critical Speed, Perturbation Equation, Dynamic Stability, Frequency Spectrum

1. Introduction

The unbalance in the rotors of rotating machinery causes vibrations and generates undesirable forces. These forces are transmitted to the machine parts and it may cause damage to the whole system. Generally, this unbalance is a result of unavoidable imperfections in rotor manufacture and assembly. Therefore, the balancing of rotors is clearly important and is accepted as fundamental requirement for the normal operation of modern low and high speed rotating machines.

*Senior Researcher, Agency for Defense Development, P.O.Box 18, Chinhae, Kyungnam 645-600, Korea

The idea of an automatic dynamic blancer, or Self-Compensating Dynamic Balancer (SCDB), has been proposed, in many forms and applications, through numerous patents to eliminate the need for balancing and yet minimize the effects of rotor unbalance and vibratory forces on the rotaing system during normal operation. The automatic dynamic balancer is usually composed of a circular disk with a groove, or race, containing spherical or cylindrical weights and low viscosity damping fluid, although early attempts used other approaches. This idea is claimed to be applicable for many applications, ranging from space vehicle components, to washing machines.

An early SCDB was proposed by the William Sellers & Co. of Philadelphia, in 1904. This company conducted a series of tests upon an experimental steam turbine incorporating an SCDB that were described by Olsen in comments on a paper by Thearle(1932). The balancer that was proposed consisted of three thin eccentric disks mounted on the shaft with the main turbine disk. The eccentric disks were a close fit on the shaft, so there would be friction between the eccentric disks and the shaft and between the disks. As the system attained its operating speed, the eccentric disks were to gradually shifted until they reached a position that brought the main disk and themselves into balance.

Between the time of this early investigation and the present at least twenty U.S. patents were granted for various types of SCDB devices that were intended for a wide range of applications. The U.S. patented devices are listed in Table 1 and no attempt has been made to list the foreign patents. The most recent U.S. patent known to the authors is that of McGale(1992). Both the apparatus and method for dynamically balancing with such inventions are extremely similar. Another common feature of these devices is the lack of both theoretical and experimental investigations into their operation.

Thearle(1932) and Den Hartog(1956) discussed why such devices would not work if a fluid was used in place of the solid weights. Alexander(1964) presented the results of a theoretical analysis of an SCDB concept. The configuration consisted of a series of counterweights in the form of spherical bearings mounted in races that were located in a long slender dynamically unbalanced spinning body. In his simulations, the system was initially at rest and was brought to its final spin rate by the application of a torque. The lateral forces due to dynamic unbalance increase until the final spin rate is reached, and then it decayed due to the action of the counterweights. However, it was not presented how the counterweights

Table 1 U.S. patents for self balancing devices since 1960

Inventor	Title	Patent No.	Year
Pierce	Automatic Wheel Balancing Device	3,006,690	1961
Salathiel	Wheel Balancer	3,164,413	1965
Colvert	Means and Methods for Balancing Wheels	3,191,997	1965
Rehnborg	Wheel Balance Correction Device	3,314,726	1967
Wesley	Dynamic Wheel Balancer	3,346,303	1967
Whitlock	Dynamic Wheel Balancer Unit	3,376,074	1968
Mitchell	Dynamic Wheel Balancer	3,376,075	1968
Foote	Ventilating Wheel Balancer	3,408,111	1968
Deakin	Automatic Balancing Device	3,410,154	1968
Mercer	Automatic Balancer	3,433,534	1969
Onufer	Balancer for Rotating Body	3,462,198	1969
Pierce	Dynamic Wheel Balancing Means	3,464,738	1969
Goodrich	Economical Automatic Balancer for Rotaing Masses	3,733,923	1973
LaBarber	Vibration Dampening Assembly	3,799,619	1974
Cobb	Dynamic Wheel and Tire Balancing Apparatus	3,913,980	1975
Cox	Automatic and Substantially Permanent Wheel Balancing Device	3,953,074	1976
Narang	Wheel and Tire Balancing System	4,269,451	1981
Kilgore	Dynamic Rotational Counterbalancer Structure	4,674,356	1987

move and how this motion is related to that of the long slender body. Cade(1965) suggested the requirements for operation of a SCDB, but the source of these suggestions is not clear

The purpose of this paper is to develop a theoretical understanding of the motion of the weights in SCDB and how this limits the operation. Many inventors have suggested various kinds of automatic dynamic balancer through U. S. patents, but they left it for others to explain why the system will work, or will not work. The motion of the weights in this interesting device is not yet understood nor well documented.

The following paper is briefly summarized as follows: in the second section the equations of motion of the balls are derived using the Lagrangian method; in section three the static and dynamic equilibria of the weights and the stability of these equilibria are discussed; some experimental results are discussed in the fourth section; and the fifth section presents the conclusions of this investigation.

2. Equations of Motion

A rotating unbalanced disk with a SCDB and supported by springs is shown in Fig. 1. The rotating disk is of mass M and the SCDB balls are each of mass m and of finite size. The point C represents the deflected centerline of the rotating system, and the point G represents the location of the mass center of the disk, not including the SCDB balls. Becuase of imperfections in the disk, its mass center G is located in a distance ε from the disk's geometric center at C. Assume that the center C of the disk is located at the origin O of the XYZ axes when the supporting springs are undeflected.

The equations of motion of this system can be derived by the Lagrangian method. If it is assumed that the disk moves only in the X and Y plane, the position vector of mass center G is expressed as

$$\bar{r}_{OG}=(X+\varepsilon\cos\psi)\hat{i}+(Y+\varepsilon\sin\psi)\hat{j} \quad (1)$$

and the position vetor of the ith ball is

$$\bar{r}_{OB}=(X+R\cos(\psi+\phi))\hat{i}$$

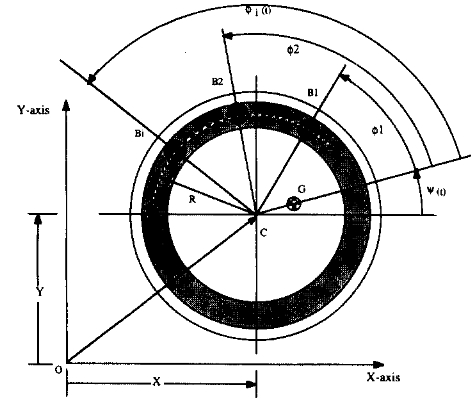

Fig. 1 Configuration of the SCDB

$$+(Y+R\sin(\psi+\phi))\hat{j} \quad (2)$$

The velocities of both the disk and ith ball are easily obtained by differentiating the Eqs. (1) and (2). Because the support springs produce forces proportional to the distance between C and O in X and Y directions and gravity acts in the negative Y direction, the Lagrangian for the system is given by

$$\begin{aligned}L=&\frac{1}{2}I_Z\dot{\psi}^2+\frac{1}{2}M[\dot{X}^2+\dot{Y}^2-2\varepsilon\dot{\psi}\dot{X}\sin\psi\\&+2\varepsilon\dot{\psi}\dot{Y}\cos\psi+\varepsilon^2\dot{\psi}^2]\\&+\frac{1}{2}\sum_{i=1}^{n}(m_i\{\dot{X}^2+\dot{Y}^2+(\dot{\phi}_i+\dot{\psi})^2R^2\\&-2R(\dot{\phi}_i+\dot{\psi})[\dot{X}\sin(\phi_i+\psi)\\&-\dot{Y}\cos(\phi_i+\psi)]\})-\frac{1}{2}k(X^2+Y^2)\\&-\sum_{i=1}^{n}m_ig[Y+R\sin(\phi_i+\psi)]\\&-MgY\end{aligned} \quad (3)$$

where I_Z is the moment of inertia of the disk about C and n is the total number of balls. The generalized coordinates for the system are chosen as

$$q=\begin{Bmatrix}X\\Y\\\psi\\\phi_1\\\phi_2\\\cdot\\\cdot\\\cdot\\\phi_n\end{Bmatrix} \quad (4)$$

The vector of generalized forces acting on the system are

$$Q=\begin{Bmatrix} -c\dot{X} \\ -c\dot{Y} \\ \tilde{M} \\ -D_1\dot{\phi}_1 \\ -D_2\dot{\phi}_2 \\ \cdot \\ \cdot \\ \cdot \\ -D_n\dot{\phi}_n \end{Bmatrix} \quad (5)$$

where c is viscous damping coefficient in the springs, $\tilde{M}$ is the moment driving the rotaing system and $D_i\dot{\phi}_i$ is the moment due to the viscous drag force acting on the ith ball.

Substituting Eqs. (3) and (5) into the Lagrange equation,

$$\frac{d}{dt}\left(\frac{\partial L}{\partial \dot{q}_j}\right)-\frac{\partial L}{\partial q_j}=Q_j \quad \text{for } j=1 \text{ to } n+3, \quad (6)$$

yields the equations of motion,

$$\left[M+\sum_{i=1}^{n}(m_i)\right]\ddot{X}+c\dot{X}+kX=M\varepsilon(\ddot{\psi}\sin\psi+\dot{\psi}^2\cos\psi)+\sum_{i=1}^{n}\{m_i[R(\ddot{\phi}_i+\ddot{\psi})\sin(\phi_i+\psi) + R(\dot{\phi}_i+\dot{\psi})^2\cos(\phi_i+\psi]\}, \quad (7)$$

$$\left[M+\sum_{i=1}^{n}(m_i)\right]\ddot{Y}+c\dot{Y}+kY=M\varepsilon(-\ddot{\psi}\cos\psi+\dot{\psi}^2\sin\psi) -\sum_{i=1}^{n}\{m_i[R(\ddot{\phi}_i+\ddot{\psi})\cos(\phi_i+\psi)-R(\dot{\phi}_i+\dot{\psi})^2\sin(\phi_i+\psi)]\}-\left[M+\sum_{i=1}^{n}(m_i)\right]g, \quad (8)$$

$$\left[I_z+M\varepsilon^2+R^2\sum_{i=1}^{n}(m_i)\right]\ddot{\psi}-\left[M\varepsilon\sin\psi+R\sum_{i=1}^{n}(m_i\sin(\phi_i+\psi))\right]\ddot{X} +\left[M\varepsilon\cos\psi+R\sum_{i=1}^{n}(m_i\cos(\phi_i+\psi))\right]\ddot{Y}+R^2\sum_{i=1}^{n}(m_i\ddot{\phi}_i)+Rg\sum_{i=1}^{n}(m_i\cos(\phi_i+\psi))=\tilde{M} \quad (9)$$

and

$$m_i[R^2(\ddot{\phi}_i+\ddot{\psi})-R\ddot{X}\sin(\phi_i+\psi)+R\ddot{Y}\cos(\phi_i+\psi)]+m_iR(\dot{\phi}_i+\dot{\psi})[\dot{X}\cos(\phi_i+\psi) +\dot{Y}\sin(\phi_i+\psi)]+Rgm_i\cos(\phi_i+\psi)=-D_i\dot{\phi}_i \quad (\text{for } i=1,2,\cdots,n) \quad (10)$$

These equations of motion can be simplified by assuming that the balls have equal mass, m, and equal coefficients for the moment of their viscous drag, D, and that the system rotates at a constant angular speed, $\dot{\psi}=\omega$. By introducing the definitions

$$\omega_n=\sqrt{\frac{k}{M}}, \quad (11)$$

$$\zeta=\frac{c}{2\sqrt{kM}} \quad (12)$$

and

$$\beta=\frac{D}{m_iR^2\omega_n} \quad (13)$$

where ω_n is the undamped natural frequency of the disk and spring system, ζ is the viscous damping factor of the disk and spring system and β is the non dimensional damping of the ball motion, the equations of motion can be written as

$$\left[1+n\frac{m}{M}\right]\frac{\ddot{X}}{\omega^2{}_n\varepsilon}+2\zeta\frac{\dot{X}}{\omega_n\varepsilon}+\frac{X}{\varepsilon} =\left(\frac{\omega}{\omega_n}\right)^2\cos(\omega t)+\frac{R}{\varepsilon}\frac{m}{M}\frac{1}{\omega_n^2}\sum_{i=1}^{n}[\ddot{\phi}_i\sin(\phi_i+\omega t)+(\dot{\phi}_i+\omega t)^2\cos(\phi_i+\omega t)], \quad (14)$$

$$\left[1+n\frac{m}{M}\right]\frac{\ddot{Y}}{\omega_n^2\varepsilon}+2\zeta\frac{\dot{Y}}{\omega_n\varepsilon}+\frac{Y}{\varepsilon} =\left(\frac{\omega}{\omega_n}\right)^2\sin(\omega t)-\frac{R}{\varepsilon}\frac{m}{M}\frac{1}{\omega_n^2}\sum_{i=1}^{n}[\ddot{\phi}_i\cos(\phi_i+\omega t)-(\dot{\phi}_i+\omega t)^2\sin(\phi_i+\omega t]-\frac{g}{\omega_n^2\varepsilon}\left[1+n\frac{m}{M}\right], \quad (15)$$

$$-\left[\frac{\varepsilon}{R}\sin\omega t+\frac{m}{M}\sum_{i=1}^{n}\sin(\phi_i+\omega t)\right]\frac{\varepsilon}{R}\frac{\ddot{X}}{\varepsilon\omega_n^2}+\left[\frac{\varepsilon}{R}\cos\omega t+\frac{m}{M}\sum_{i=1}^{n}\cos(\phi_i+\omega t)\right]\frac{\varepsilon}{R}\frac{\ddot{Y}}{\varepsilon\omega_n^2} +\frac{1}{\omega_n^2}\frac{m}{M}\sum_{i=1}^{n}\ddot{\phi}_i=\frac{\tilde{M}}{MR^2\omega_n^2} \quad (16)$$

and

$$\frac{\ddot{\phi}_i}{\omega_n^2}-\frac{1}{\omega_n^2}\frac{\ddot{X}}{R}\sin(\phi_i+\omega t)+\frac{1}{\omega_n^2}\frac{\ddot{Y}}{R}\cos(\phi_i+\omega t)+\frac{1}{\omega_n^2 R}(\dot{\phi}_i+\omega)[\dot{X}\cos(\phi_i+\omega t)$$
$$+\dot{Y}\sin(\phi_i+\omega t)]+\frac{g}{\omega_n^2 R}\cos(\phi_i+\omega t)=-\beta\frac{\dot{\phi}_i}{\omega_n} \tag{17}$$

With the assumptions made above, the unknowns in these equations are X, Y, $\tilde{M}$ and ϕ_i for i=1 to n. Since there is little interest in the moment $\tilde{M}$ that is needed to drive the system, Eq. (16) will not be considered further. The system is then governed by n+2 coupled nonlinear ordinary differential equations. The non dimensional motion of the system, as given by X/ε, Y/ε and ϕ_i, is a function of non dimensional time ω_nt and the seven parameters, n, m/M, ω/ω_n, ε/R, ζ, β and $g/(\omega_n^2\ \varepsilon)$. The next section considers some simple solutions of these equations.

3. Static and Dynamic Equilibria and Their Stability

If gravitational effects can be ignored, steady solutions can be easily obtained. When the balls have reached an equilibrium position, $X=\dot{X}=\ddot{X}=0$, $Y=\dot{Y}=\ddot{Y}=0$ and $\dot{\phi}_i=\ddot{\phi}_i=0$. In this case Eq. (17) is satisfied, and Eqs. (14) and (15) yield, after some rearrangement,

$$\frac{\varepsilon}{R}+\frac{m}{M}\sum_{i=1}^{n}\cos\phi_i=0 \tag{18}$$

and

$$\sum_{i=1}^{n}\sin\phi_i=0. \tag{19}$$

These equations simply state that the combined center of mass of the system must be on the axis of rotation(provided ε/R is less than or equal to n m/M) to obtain this vibration-free solution, as would be expected.

A dynamic, steady state solution is obtained by assuming that the balls are positioned at fixed but steady locations with $\dot{\phi}_i=\ddot{\phi}_i=0$. To investigate this case it is useful to make use of complex notation where $Z=X+i$Y. Multiplying Eq. (15) by i and adding it to Eq. (14) gives an equation for the complex displacement Z,

$$\left[1+n\frac{m}{M}\right]\frac{\ddot{Z}}{\omega_n^2\varepsilon}+2\zeta\frac{\dot{Z}}{\omega_n\varepsilon}+\frac{Z}{\varepsilon}$$
$$=C_1e^{i(\omega t+\alpha)}, \tag{20}$$

where

$$C_1=\frac{R}{\varepsilon}\left(\frac{\omega}{\omega_n}\right)^2\sqrt{\left(\frac{\varepsilon}{R}+\frac{m}{M}\sum_{i=1}^{n}\cos\phi_i\right)^2+\left(\frac{m}{M}\sum_{i=1}^{n}\sin\phi_i\right)^2} \tag{21}$$

and

$$\alpha=\tan^{-1}\left\{\frac{\frac{m}{M}\sum_{i=1}^{n}\sin\phi_i}{\frac{\varepsilon}{R}+\frac{m}{M}\sum_{i=1}^{n}\cos\phi_i}\right\} \tag{22}$$

Notice that if the system is balanced, so that Eqs. (18) and (19) hold, C_1 is zero and the steady solution for Z is also zero. If the system is not balanced then C_1 describes the imbalance and the steady solution of Eq. (20) is

$$Z=\frac{RC_1}{C_2}e^{i(\omega t+\alpha-\zeta)}, \tag{23}$$

where C_2 is the usual magnification factor (including the mass of the balls),

$$C_2=\sqrt{\left\{1-\left[1+n\frac{m}{M}\right]\left(\frac{\omega}{\omega_n}\right)^2\right\}^2+\left\{2\zeta\frac{\omega}{\omega_n}\right\}^2} \tag{24}$$

and

$$\zeta=\tan^{-1}\left\{\frac{2\zeta\frac{\omega}{\omega_n}}{1-\left[1+n\frac{m}{M}\right]\left(\frac{\omega}{\omega_n}\right)^2}\right\} \tag{25}$$

The motion of the disk is determined by the position of the balls, as given by Eqs. (23), (24) and (25) and the position of the balls is determined by Eq. (17). Extracting both X and Y from

Eq. (20), substituting these results into Eq. (17) and making use of some identities yields

$$C_1\sin(\phi_i-\alpha+\zeta)=0. \tag{26}$$

The most interesting solution to Eq. (26) is the case when the system is balanced, when Eqs. (18) and (19) are satisfied, making C_1 zero. Clearly other solutions exist where $\sin(\phi_i-\alpha+\zeta)$ is zero. One of these other solutions is shown in Fig. 2. In obtaining these steady solutions no consideration has been given to how they are reached and none will be given here. However, the stability of the balanced solution will be investigated next.

To investigate the stability of the solutions of Eqs. (14), (15) and (17) a perturbation approach is used. Suppose that the balls have some slight displacement from their dynamic equilibrium position, ϕ_{si}. Let

$$\phi_i=\phi_{si}+\delta\phi_{1i}+\kappa, \tag{27}$$

$$X=X_0+\delta X_1+\kappa, \tag{28}$$

and

$$Y=Y_0+\delta Y_1+\kappa \tag{29}$$

where δ is a small quantity and i=1, 2,..., n.

Substituting Eqs. (27), (28) and (29) into Eqs. (14), (15) and (17), dropping terms of order δ^2 or higher order, making small angle approximations, equating terms by the power of δ and assuming that ϕ_{si} satisfies Eqs. (18) and (19), the position that balances the system, gives two sets of equations. The δ^0 equations have the steady solutions $X_o=Y_o=0$ and ϕ_{si}. The δ^1 equations are given by

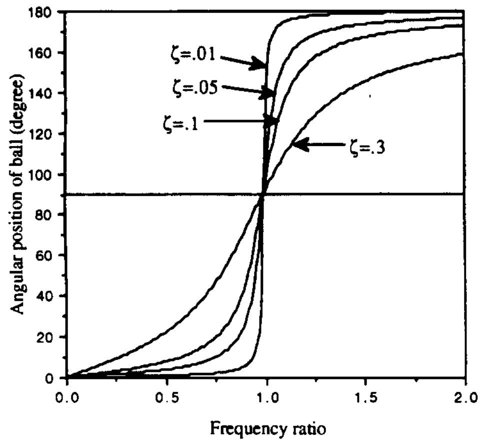

Fig. 2 Angular positon of the balls as a function of frequency ratio for m/M=0.005 and ε/R=0.005

$$(1+n\tilde{m})\ddot{\tilde{X}}_1+2\zeta\dot{\tilde{X}}_1+\tilde{X}_1 =\tilde{m}\tilde{R}\sum_{i=1}^{n}\{\ddot{\phi}_{1i}\sin(\phi_{si}+\tilde{\omega}\tilde{t})+2\tilde{\omega}\dot{\phi}_{1i}\cos(\phi_{si}+\tilde{\omega}\tilde{t})-\tilde{\omega}^2\phi_{1i}\sin(\phi_{si}+\tilde{\omega}\tilde{t})\} \tag{30}$$

$$(1+n\tilde{m})\ddot{\tilde{Y}}_1+2\zeta\dot{\tilde{Y}}_1+\tilde{Y}_1 =\tilde{m}\tilde{R}\sum_{i=1}^{n}\{\ddot{\phi}_{1i}\cos(\phi_{si}+\tilde{\omega}\tilde{t})-2\tilde{\omega}\dot{\phi}_{1i}\sin(\phi_{si}+\tilde{\omega}\tilde{t})-\tilde{\omega}^2\phi_{1i}\cos(\phi_{si}+\tilde{\omega}\tilde{t})\} \tag{31}$$

and

$$\ddot{\phi}_{1i}-\ddot{\tilde{X}}_1\sin(\phi_{si}+\tilde{\omega}\tilde{t})+\ddot{\tilde{Y}}_1\cos(\phi_{si}+\tilde{\omega}\tilde{t})+\tilde{\omega}\dot{\tilde{X}}_1\cos(\phi_{si}+\tilde{\omega}\tilde{t})+\tilde{\omega}\dot{\tilde{Y}}_1\sin(\phi_{si}+\tilde{\omega}\tilde{t})=-\beta'\dot{\phi}_{1i} \tag{32}$$

in non dimensional form, where X_1 and Y_1 have been nondimensionalized by ε, time by ω_n, and $\tilde{\omega}=\omega/\omega_n$, $\tilde{R}=\varepsilon/R$, $\tilde{m}=m/M$ and $\beta'=\beta/\omega_n$. Although linear, Eqs. (30), (31) and (32) have time varying coefficiernts and no closed form solution appears possible. Floquet theory has been developed for characterizing the functional behavior of linear ordinary differential equations with periodic coefficients. The general Floquet theory is analytical, but a numerical version will be outlined here.

Equations (30) to (32) can be written in state variable form

$$\dot{\eta}=\mathrm{A}(t)\,\eta \tag{33}$$

where the vetor η is made up of $\dot{\tilde{X}}_1$, $\tilde{X}_1$, Y_1, $\dot{\tilde{Y}}$, ϕ_1, ϕ_2,..., $\dot{\phi}_1$, $\dot{\phi}_2$,... To apply Floquet Theory, Euler integration is used to find a matrix solution of the equation

$$\dot{\mathrm{U}}=\mathrm{A}(t)\,\mathrm{U} \tag{34}$$

where U is a matrix, with initial conditions

$$\mathrm{U}(0)=\mathrm{I} \tag{35}$$

where I is the identity matrix, to a time equal to

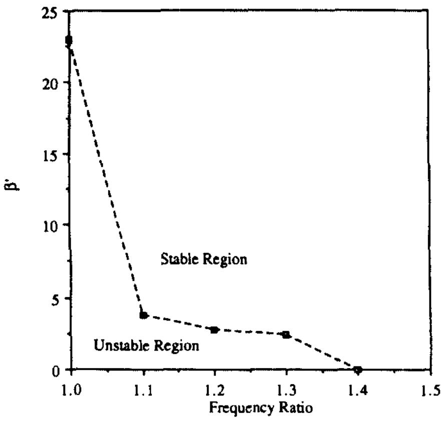

Fig. 3 Stability of the balanced solution with one ball, m/M=0.005 and ζ=0.01

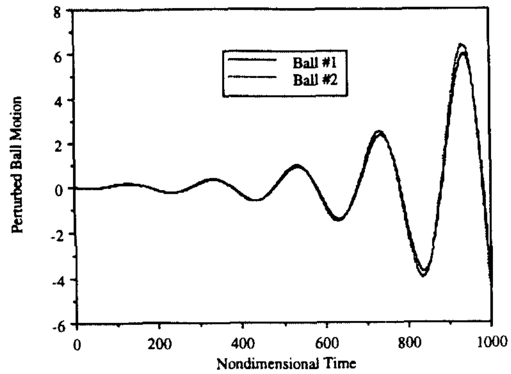

Fig. 5 Growth of the perturbation of the positon of both balls with time, ω/ω_n=1.0, m/M=0.005, ε/R=0.001, and β'=0.01

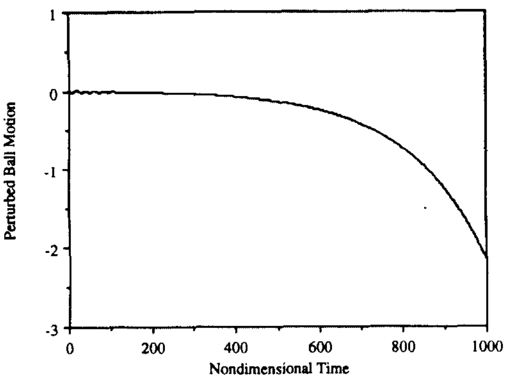

Fig. 4 Growth of the perturbation of the position of one ball with time, ω/ω_n=0.7, m/M=0.005, ε/R=0.001, and β'=0.01

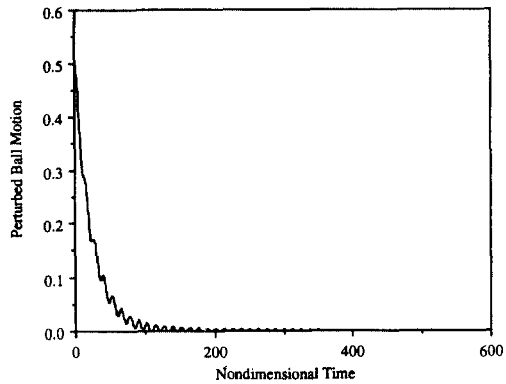

Fig. 6 Stability of the motion of one ball versus time, ω/ω_n=1.5, m/M=0.005, ε/R=0.001, and β'=0.01

the period of the oscillatory coefficients, T. The complex eigenvalues of the matrix U(T) are then determined. If the magnitudes of all these eigenvalues are less than unity the system is asymptotically stable. If one or more of the eigenvalues has a magnitude greater than unity the system is unstable. Figure 3 shows a result of such a set of calculations for one ball, with m/M =0.005, ζ=0.01 and $\phi_{si}=\pi$, the offset of the center of gravity of the disk was chosen so the single ball would balance the system in this location. Notice that as the critical speed is approached, increasing damping of the ball motion is required for a stable solution. Above a frequency ratio of approximately 1.4, damping is not required for stable solutions. Below critical speed no stable solutions could be found for $\phi_{si}=\pi$ independent of ball damping. More detail of these calculations is given by Lee(1993).

Ball position was also determined by numerical integration of the perturbation Eqs. (30) to (32) with two balls. Although not conclusive in defining the motion, these results are in general agreement with the results described above. Figures 4 to 6 are examples of these results. In Fig. 4(ω/ω_n =0.7) the balls move steadily away from the balanced position. Figure 5 shows a growing oscillatory motion of the balls away from the balanced position for ω/ω_n=1.0. Figure 6 shows the stability of the balls for ω/ω_n=1.5.

4. Experimental Results

In additon to the analytical investigation, a brief experimental investigation was undertaken. The apparatus consisted of a 1.35m long shaft 2. 54cm(1 in) in diameter mounted in self-aligning bearings and driven by a variable speed D.C. motor through a flexible coupling. A clear plastic disk with a 0.953cm(3/8 in) diameter race was centered between the bearings. Steel ball bearings 0.873cm(11/32 in) could be loaded into the race along with mineral oil, to act as a damping fluid, through a. 0.953cm(3/8 in) hole in the disk. This hole shifted the center of gravity of the disk from the axis of the shaft. The mean radius of the race from the shaft center was 5.238cm($2\frac{1}{16}$ in). The entire system was mounted vertically to minimize gravitational effects, see Fig. 7. Modal analysis was applied to the non-rotating system to estimate the critical speeds of the system. The first critical speed was found to be 25.4 Hz or 1524 RPM, higher natural frequencies were found at 106 Hz, 6396 RPM, and 213 Hz, 12,826 RPM. An accelerometer was mounted on one of the bearing caps and video and still cameras were used in conjunction with a strobe light to record the ball positions with the shaft rotating.

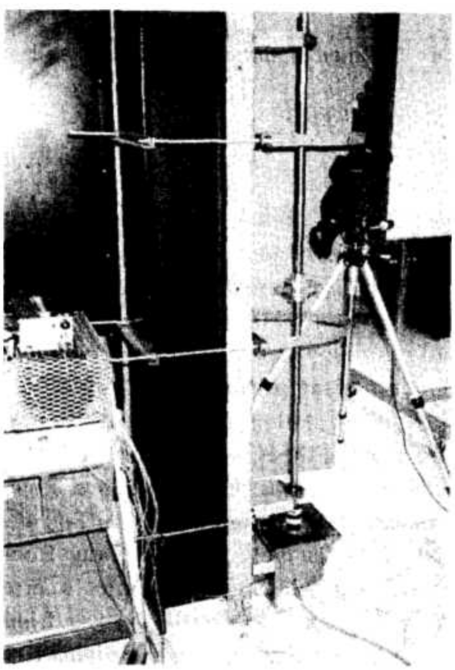

Fig. 7 Experimental apparatus

An example of the vibration spectra obtained with and without balls in the race is shown in Fig. 8 with the system running at 1000 RPM, 16.

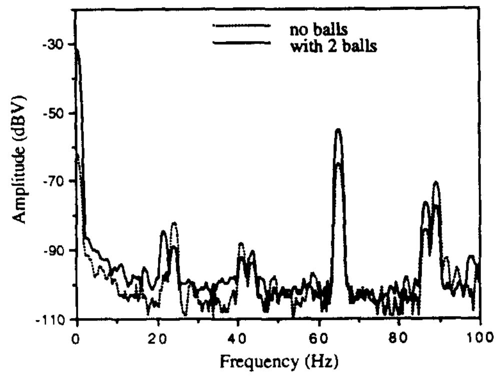

Fig. 8 Vibration spectra at the bearing at 1000 RPM, with and without balls in the SCDB

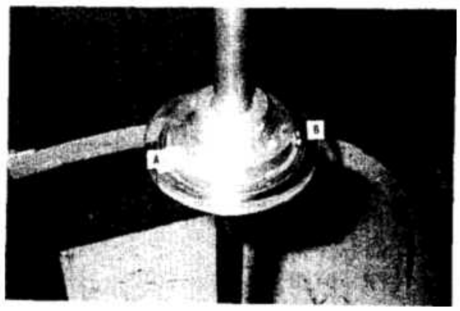

Fig. 9 Position of the balls in the SCDB at 1000 RPM, "A" is light side of the disk, "B" is the position of the balls

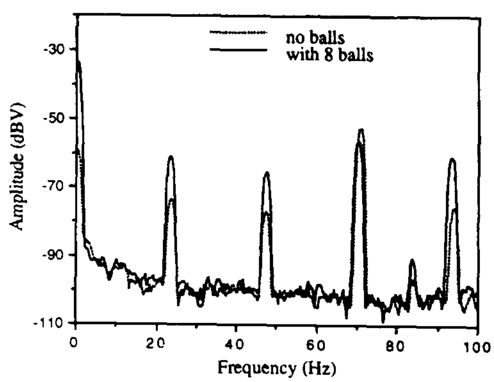

Fig. 10 Vibration spectra at the bearing at 1420 RPM, with and without balls in the SCDB

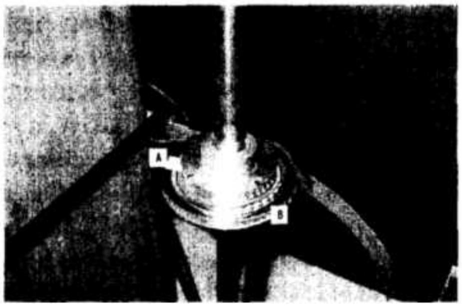

Fig. 11 Position of the balls in the SCDB at 1420 RPM, "A" is light side of the disk, "B" is the position of the balls

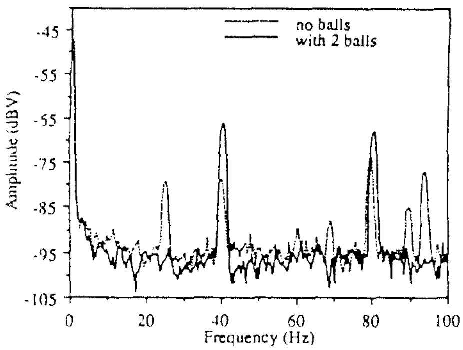

Fig. 12 Vibration spectra at the bearing at 2400 RPM, with and without balls in the SCDB

7 Hz, well below the critical speed. Only a low level of vibration is seen at 16.7 Hz without balls in the race, but the level is increased by the presence of the two balls. A significant vibration level is seen at near 25.4 Hz without the ball in the race and the level is decreased by the addition of the balls. However the vibration level is increased at a frequency of about 22 Hz. Figure 9 shows the position of the balls in the race, approximately 180° from the light side of the disk, $\phi=0^\circ$, as would be expected. The origin of the other spectral peaks is not understood, but is likely due to other natural frequencies in the structure.

The system could not be run at the critical speed due to the large deflection that occurred. The rotation speed closest to the critical speed that was investigated was 1420 RPM, 23.7 Hz, or an ω/ω_n of .93. In this case eight balls were used in the race and most spectral peaks were increased

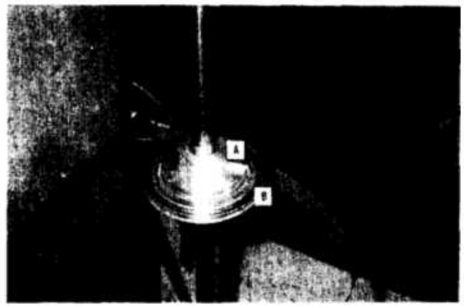

Fig. 13 Position of the balls in the SCDB at 2400 RPM, "A" is light side of the disk, "B" is the position of the balls

by the presence of the balls, see Fig. 10. The position of the balls is seen in Fig. 11, at an angle of about 150° from the light side of the disk, or $\phi=30^\circ$. The observed value of ϕ is obtained from Eq. (27) with a structural damping, ζ, between 0.01 and 0.03.

The vibration spectrum at a rotation speed of 2400 RPM, 40 Hz, is shown in Fig. 12. The presence of two balls in the race nearly eliminates the signal at the critical speed but increases the vibration level at the rotational frequency. This effect is also observed with a large number of balls. Figure 13 shows the position of the balls, with ϕ near 180°, as anticipated.

5. Conclusions

The general pupose of the study of rotor dynamics is to increase understanding of rotor vibration phenomena and thus provide means for controlling or eliminating these vibrations. As mentioned previously, the purpose of this research is to better understand the operation and ball motion in a Self-Compensating Dynamic Balancer(SCDB) and understand the limitations in using a SCDB. Many inventors have suggested various kinds of automatic dynamic balancer through U.S. patents, but they left it for others to explain why this system will work or will not work with solid balls and damping fluid that has a low viscosity. To the author's knowledge, the motion analysis of the balls and the rotating shaft as presented in this paper discusses the first attempt to analyze the dynamics of an automatic dynamic balancer with solid balls and damping fluid. From the preceding work, the following results were obtained:

(1) The equations of motion of the balls were derived by the Lagrangian method. Static and dynamic solutions were derived from the analytic model. Perturbation solutions were also obtained from the analytic model. To investigate dynamic stability of the perturbed motion two different methods, i.e., the Floquet theory with only one ball and direct computer simulation, were conducted. On the basis of on the results of stability investigation, ball positions that result in a balanced system are stable above the critical speed for $\beta'=3.8$. At critical speed the position is seen to be stable for β' greater than 23. However, the balanced position is unstable below critical speed for all β'.

(2) To understand the motion of the balls and rotating disk, numerical simulations were carried out. These results support the conclusions given above, that if the rotating system operates above the first critical speed, the balls can balance the rotating system. At the first critical speed, the equilibrium of the system depends on the damping coefficient between the balls and the race. Large damping coefficients can balance the system. Below the first critical speed, the balls can not balance the system in any case.

(3) In order to evaluate the true merits of the SCDB, it is necessary to apply it to the actual rotor system. To be credible, the SCDB must have, in addition to theoretical appeal, demonstrated practical appeal. That is, it is necessary to demonstrate its effectiveness in an actual rotor system. To investigate the ball motion and to determine how this ball motion is related to the rotating shaft, experiments were conducted. On the basis of the results of these experiments, when the system operates below the first critical speed the balls are positioned on the side near the center of gravity of the system and increase the imbalance in the system. When the system operates near the first critical speed the balls also do not balance the system. When the system operates above the first critical speed the balls positon themselves so they can balance the system. In this case the balls are positioned on the opposite side from the center of gravity of the system. All these experimental results are consistent with theoretical and numerical results.

However, there are several limitations in using a SCDB. A single set of the SCDB is sufficient to effectively cancel the system imbalance in a rotating shaft that is uniform along its length and a large portion of the imbalance is radial displacement of the center of gravity from the axis of rotation. However, based on the experimental approach, the rotating system must be dynamically balanced to a fairly close tolerance before the SCDB is effective. If the SCDB is intended for use in a complicated rotating system, and there is no way to predict the amount of imblance, it is very difficult to determine the ball mass and the dimensions needed for the SCDB.

References

Alexander, J. D., 1964, "An Automatic Dynamic Blancer," *Proceeding, 2nd Southeastern Conference*, pp. 415~426.

Cade, J. W., 1965, "Self-Compensating Balancing in Rotating Mechanisms," *Design News*, pp. 234~239.

Den Hartog, J. P., 1956, *Mechanical Vibrations*, Dover, New York, pp. 225~281.

Hahn, W., 1967, *Stability of Motion*, Springer-Verlag, New York.

Lee, J., 1993, "Theoretical and Experimental Analysis of Self-Compensating Dynamic Balancer in a Rotating Mechanism," Ph. D. Dissertation, Mechanical Engineering Department, University of Utah, Salt Lake City, UT 84112, U.S.A.

McGale, P.J., 1992, "Apparatus for Dynamical Balancing of Rotaing Objects and Method for Making Same," U.S. Patent 5, 142, 936, Washington.

Nayfeh. A.H. and Mook, D.T., 1979, *Nonlinear Oscillations*, Wiley, New York, pp. 273~283.

Thearle, E.L., 1932, "A New Type of Dynamic-Balancing Machine," *Transactions of the ASME*, Vol. 54, APM-54-12, pp. 131~141.

Notes upon Balancing High-Speed Machinery, 1904, *Railway Machinery*, pp. 183~184.